Research Article

Author for correspondence:
Lei-Lei Gao. Center for Reproductive Medicine, Department of Gynecology, Zhejiang Provincial People's Hospital, Affiliated People's Hospital, Hangzhou Medical College, Hangzhou, Zhejiang, China 310014.
E-mail: gaoleilei198802@126.com

*These authors contributed equally to this work.

CAMBRIDGE
UNIVERSITY PRESS

ZP3 and AIPL1 participate in GVBD of mouse oocytes by affecting the nuclear membrane localization and maturation of farnesylated prelamin A

Zhen Jin[1],*, Qing-Mei Yang[1],*, Chen-Yu Xiao[2] and Lei-Lei Gao[2]

[1]Center for Reproductive Medicine, Department of Reproductive Endocrinology, Zhejiang Provincial People's Hospital, Affiliated People's Hospital, Hangzhou Medical College, Hangzhou, Zhejiang, China 310014 and [2]Center for Reproductive Medicine, Department of Gynecology, Zhejiang Provincial People's Hospital, Affiliated People's Hospital, Hangzhou Medical College, Hangzhou, Zhejiang, China 310014

Summary

The low maturation rate of oocytes is an important reason for female infertility and failure of assisted pregnancy. The germinal vesicle breakdown (GVBD) is a landmark event of oocyte maturation. In our previous studies, we found that zona pellucida 3 (ZP3) was strongly concentrated in the nuclear region of germinal vesicle (GV) oocytes and interacted with aryl hydrocarbon receptor-interacting protein-like 1 (AIPL1) and lamin A to promote GVBD. In the current study, we found that lamin A is mainly concentrated in the nuclear membrane. When ZP3 is knocked down, lamin A will be partially transferred to the nucleus of oocytes. The prelamin A is increased in both the nuclear membrane and nucleus, while phosphorylated lamin A (p-lamin A) is significantly reduced. AIPL1 was also proved to accumulate in the GV region of oocytes, and ZP3 deletion can significantly inhibit the aggregation of AIPL1 in the nuclear region. Similar to ZP3 knockdown, the absence of AIPL1 resulted in a decrease in the occurrence of GVBD, an increase in the amount of prelamin A, and a significant decrease in p-lamin A in oocytes developed *in vitro*. Finally, we propose the hypothesis that ZP3 can stabilize farnesylated prelamin A on the nuclear membrane of AIPL1, and promote its further processing into mature lamin A, therefore promoting the occurrence of GVBD. This study may be an important supplement for the mechanism of oocyte meiotic resumption and provide new diagnostic targets and treatment clues for infertility patients with oocyte maturation disorder.

Introduction

The meiosis of oocytes starts as early as the primordial germ cells migrating to the reproductive ridge in the embryonic stage, and stops at the diploid stage, also known as the germinal vesicle (GV) stage. From the time the fetus is born to the time of adolescence, the first follicles are raised and developed. The luteinizing hormone (LH) peak before ovulation induces oocyte meiotic resumption that starts from germinal vesicle breakdown (GVBD), and then stops at the second meiosis stage (MII stage) after two successive meioses. After fertilization, the mature MII oocytes will continue to complete the second meiosis. It can be seen that the meiotic recovery of oocytes, namely GVBD, is the key event of oocyte maturation. At present, the specific molecular events and regulatory mechanisms of GVBD in oocytes have not been fully elucidated. An in-depth study of the molecular mechanism of GVBD is an urgent problem in the field of reproductive medicine, which is of great practical significance for the diagnosis and treatment of female infertility.

At present, the specific molecular events and regulatory mechanisms of GVBD in oocytes have not been fully elucidated. The mainstream views include the following processes and aspects. First, endogenous oocyte factors and the granulosa cell signalling pathway activate oocyte maturation promoting factor (MPF) and induce GVBD. Then, the activated MPF induces GVBD mainly by promoting the phosphorylation of lamin, leading to depolymerization of the nuclear fibre layer and rupture of the nuclear membrane. Lamins (including A, B, C) are important components of the nuclear fibre layer. In the cell cycle, when lamin is phosphorylated, the nuclear fibre layer depolymerizes and the nuclear membrane cleaves. In mitotic cells, lamin exists in the cytoplasm in the form of a monomer. When lamin is dephosphorylated, the nuclear fibre layer will repolymerize and the nuclear membrane recombines (Dechat *et al.*, 2008; Taimen *et al.*, 2009; Moiseeva *et al.*, 2016; Mehsen *et al.*, 2018). Lamin is the direct substrate of MPF. When MPF in oocytes is activated, lamin A/C accurately located in the nuclear membrane is phosphorylated at the 22nd and 392nd serine by MPF catalysis. The phosphorylated lamin A/C

causes the nuclear fibre layer to depolymerize and the nuclear membrane breaks down immediately (Peter *et al.*, 1990, 1991; Dessev *et al.*, 1991; Adhikari *et al.*, 2012).

ZP3 is an important component of the zona pellucida of oocytes. It can act as a primary sperm receptor and induce acrosome reactions during fertilization (Gupta, 2018; Wassarman and Litscher, 2018). ZP3 knockout mice lose fertility completely and their oocytes show obvious morphological abnormalities (Liu *et al.*, 1996). At present, there is no in-depth study on other biological functions of ZP3 except as a zona pellucida component. Our previous studies found that ZP3 was not only located in the zona pellucida, but also strongly concentrated in the nuclear region in GV oocytes. In GVBD and subsequent oocytes, it decreased significantly around the chromosome (Gao *et al.*, 2017). When ZP3 was knocked down with specific siRNA, oocytes showed obvious developmental disorder, and the proportion of arrest in the GV phase increased significantly, suggesting that ZP3 may play an important role in the occurrence of GVBD (Gao *et al.*, 2017). We performed immunoprecipitation (IP) experiments on ZP-free oocytes, and detected possible interacting proteins including aryl hydrocarbon receptor-interacting protein-like 1 (AIPL1) and lamin A. AIPL1 is very important for the stability and presence of farnesylated proteins, this can avoid protein degradation and promote their further processing (Ramamurthy *et al.*, 2004). Whether AIPL1 regulates the farnesylation of prelamin A and how ZP3 participates in this process are unknown. Whether ZP3 can affect the recovery process of oocyte meiosis through these molecular effects also needs further study.

Materials and methods

General chemicals, reagents cells and animals

Unless otherwise specified, chemicals and reagents were purchased from Sigma-Aldrich and Merck KGaA. The 265 3-week-old female specific pathogen-free ICR mice (weighing 18–20 g) used in this study were obtained from Vital River Experimental Animal Technical Co., Ltd. Animals were housed at a temperature of 20–26°C and a humidity of 40–70% with a 12 h light/dark cycle. The mice were fed in feeding boxes, and the frequency of food replacement was two times a week, and the frequency of water bottle replacement was three times a week. All animal experiments were approved by the Animal Protection and Utilization Committee of Nanjing Medical University (Nanjing, China) and conducted in accordance with institutional guidelines.

Antibodies

Rabbit polyclonal ZP3 (H-300) (cat. no. sc-25802) was purchased from Santa Cruz (Dallas, Texas, USA). Rabbit anti-ZP3 (cat. no. AV35855) was purchased from Sigma (St. Louis, MO, USA). Mouse monoclonal anti-β-actin (cat. no. A5316-100) antibody was obtained from Sigma-Aldrich, Merck KGaA. Mouse monoclonal anti-lamin A (133A2) (cat. no. ab8980) antibodies were purchased from Abcam, Inc. Goat polyclonal prelamin A (C-20) (cat. no. sc-6214) was purchased from Santa Cruz (Dallas, Texas, USA). Mouse monoclonal anti-lamin C (EM-11) (cat. no. NBP1-50051PE) antibodies were purchased from Novus Biologicals, Inc., rabbit anti-AIPL1 (cat. no. 15108-1-AP) was purchased from Proteintech (Chicago, Illinois, USA). Mouse monoclonal anti-CDK1 (cat. no. 33-1800) antibodies were purchased from Invitrogen and Thermo Fisher Scientific, Inc. Rabbit polyclonal anti-phospho-CDK1 (Thr161) was purchased from Beyotime,

Inc. Mouse monoclonal anti-cyclin B (D-1) (cat. no. sc-166210) antibodies were purchased from Santa Cruz Biotechnology, Inc. Rabbit polyclonal anti-phospho-cyclin B1 (Ser133) was purchased from Hushi Medicine Technology, Inc. Mouse monoclonal anti-β-tubulin (cat. no. sc-5274) antibodies were purchased from Santa Cruz Biotechnology, Inc. Rabbit polyclonal anti-β-actin (cat. no. 30102ES40) was purchased from Yeasen Biotech Co., Ltd. Cy2-conjugated donkey anti-mouse IgG (code no. 715-225-150), rhodamine (TRITC)-conjugated donkey anti-goat IgG (code no. 705-025-147), and Alexa Fluor 647-conjugated donkey anti-human IgG (code no. 709-605-149) were purchased from the Jackson ImmunoResearch Laboratories, Inc. Horseradish peroxidase (HRP)-conjugated rabbit anti-goat IgG (cat. no. 31402) and HRP-conjugated goat anti-mouse IgG (cat. no. 31430) were purchased from Invitrogen, Thermo Fisher Scientific, Inc.

Oocyte collection and culture

Immature oocytes at the GV stage were obtained from the ovaries of 3-week-old female ICR mice. The mice were euthanized with carbon dioxide. The ovaries were removed and placed in HEPES containing 2.5 nm milrinone and 10% FBS (Gibco, Thermo Fisher Scientific, Inc.). The follicle was punctured by injection acupuncture and oocytes were washed out from the cumulus–oocyte complex. In total, 50 separated shelled oocytes were placed in 100-μl culture medium drops, under the mineral oil in plastic containers (BD Biosciences). The medium was MEM+ [containing 0.01 mm EDTA, 0.23 mm Na-pyruvate, 0.2 mm penicillin/streptomycin, 3 mg/ml bovine serum albumin (BSA) and 20% FBS]. The oocytes were cultured at 37.0°C, 5% O_2 and 5% CO_2. Before *in vitro* maturation (IVM), 2.5 nM milrinone was added to all media to prevent meiosis recovery.

siRNA production and microinjection

Table 1 and Table 2 list the sequences of all DNA templates used to produce siRNA for ZP3 and AIPL1, respectively. The sequence of the control template is a simulated sequence and does not specifically bind to any mRNA in the mouse genome. By blocking the DNA template of four different DNA coding regions (amino acid sequence coding in protein, CDS) of ZP3 and AIPL1 mRNA, the template was designed online through BLOCK-iT™ RNAi Designer (http://rnaidesigner.invitrogen.com/rnaiexpress/) with some modifications. Sequence specificity was verified by a BLAST (http://blast.ncbi.nlm.nih.gov/Blast.cgi) homology search.

siRNAs were made using the T7 RiboMAX™ Express RNAi System (Promega Corporation), according to the manufacturer's instructions. In short, for a double-stranded siRNA in four ZP3 and AIPL1 CDS regions, two pairs of synthesized complementary single-stranded DNA oligonucleotides were first annealed to form two double-stranded DNA templates. Then, two complementary single-stranded siRNA were synthesized according to the two templates and annealed to form the final double-stranded siRNA. Next, the siRNA was purified by conventional phenol/chloroform/isopropanol precipitation, and then checked on the agarose gel. The siRNA was then calibrated and stored at −80°C. A ready-to-use siRNA mixture was prepared by mixing siRNA with four targets at an equal molar ratio of 5 μm to the final concentration.

Microinjection of siRNA into the cytoplasm of fully grown immature oocytes was used to knock down ZP3 and AIPL1. After injection, oocytes were arrested at the GV stage with 2.5 μM milrinone for 20 h, and then were cultured in milrinone-free M2 medium for maturation.

Table 1. DNA oligos for siRNA production

Target site	DNA templates
ZP3 CDS 133–153[a]	Oligo 1: GGATCCTAATACGACTCACTATAGAGTGTCTGGAAGCTGAACTA[b]
	Oligo 2: AATAGTTCAGCTTCCAGACACTCTATAGTGAGTCGTATTAGGATCC[b]
	Oligo 3: GGATCCTAATACGACTCACTATA TAGTTCAGCTTCCAGACACTC[b]
	Oligo 4: AAGAGTGTCTGGAAGCTGAACTATATAGTGAGTCGTATTAGGATCC[b]
ZP3 CDS 387–407[a]	Oligo 1: GGATCCTAATACGACTCACTATAGACTAACCGTGTGGAGGTACC[b]
	Oligo 2: AAGGTACCTCCACACGGTTAGTCTATAGTGAGTCGTATTAGGATCC[b]
	Oligo 3: GGATCCTAATACGACTCACTATAGGTACCTCCACACGGTTAGTC[b]
	Oligo 4: AAGACTAACCGTGTGGAGGTACCTATAGTGAGTCGTATTAGGATCC[b]
ZP3 CDS 727–747[a]	Oligo 1: GGATCCTAATACGACTCACTATAGATGGTCTATCTGAGAGCTTT[b]
	Oligo 2: AAAAAGCTCTCAGATAGACCATCTATAGTGAGTCGTATTAGGATCC[b]
	Oligo 3: GGATCCTAATACGACTCACTATAAAAGCTCTCAGATAGACCATC[b]
	Oligo 4: AAGATGGTCTATCTGAGAGCTTTTATAGTGAGTCGTATTAGGATCC[b]
ZP3 CDS 940–960[a]	Oligo 1: GGATCCTAATACGACTCACTATAGAGGGTGATGCTGACATCTGT[b]
	Oligo 2: AAACAGATGTCAGCATCACCCTCTATAGTGAGTCGTATTAGGATCC[b]
	Oligo 3: GGATCCTAATACGACTCACTATAACAGATGTCAGCATCACCCTC[b]
	Oligo 4: AAGAGGGTGATGCTGACATCTGTTATAGTGAGTCGTATTAGGATCC[b]
Control[c]	Oligo 1: GGATCCTAATACGACTCACTATACCTACGCCACCAATTTCGTTT[b]
	Oligo 2: AAAAACGAAATTGGTGGCGTAGGTATAGTGAGTCGTATTAGGATCC[b]
	Oligo 3: GGATCCTAATACGACTCACTATAAAAACGAAATTGGTGGCGTAGG[b]
	Oligo 4: AACCTACGCCACCAATTTCGTTTTATAGTGAGTCGTATTAGGATCC[b]

[a]The numbers are the starting and ending positions of the target sites in ZP3 CDS (NM_011776.1 in NCBI).
[b]Two pairs of DNA oligos are required for each double-stand siRNA. Oligo 2 is complementary with oligo 1 except for an 'AA' overhang at the 5′ end; Oligo 3 is complementary with oligo 4 except for an 'AA' overhang at the 5′ end. In each oligo, gene-specific sequences are underlined, other sequences are for recognition and binding by T7 RNA polymerase.
[c]Control siRNA does not target to any mRNA sequence in mouse.

Immunofluorescence

The oocytes were washed in PBS with 0.05% polyvinylpyrrolidone (PVP) for a short time, then infiltrated in 0.5% Triton X-100/PHEM (60 mM PIPES, 25 mM HEPES pH 6.9, 10 mM EGTA, 8 mM $MgSO_4$) for 5 min, and washed in PBS/PVP three times. Then, the oocytes were fixed in 3.7% PFA/PHEM for 20 min at room temperature, washed in PBS/PVP three times (10 min each time), and blocking buffer (1% BSA/PHEM with 100 mM glycine) was used at room temperature. The oocytes were incubated overnight at 4°C with a primary antibody diluted in blocking buffer, washed three times (10 min each time) in PBS with 0.05% Tween-20 (PBST), incubated in closed buffer for 45 min with a secondary antibody diluted in blocking buffer (1:750 in all cases) and washed three times (10 min each time) in PBST. Finally, the oocytes were stained with 10 μg/ml Hoechst 33258 (Sigma-Aldrich; Merck KGaA) at room temperature for 10 min. Then the oocytes were installed on a slide with mounting medium (0.5% propyl gallate, 0.1 M Tris–HCl, pH 7.4, 88% glycerol) and covered with a layer of glass (thickness 0.13–0.17 μm). To maintain the dimension of oocytes, two double-sticky bands (90 μm thick) were placed between the slide and the cover slide. The main antibodies were diluted as follows: anti-ZP3 (cat. no. sc-25802, Santa Cruz Biotechnology, Inc.), 1:200; anti-lamin A (133A2) (cat. no. ab8980), 1:200; anti-prelamin A (C-20) (cat. no. sc-6214), 1:200; anti-lamin C (EM-11) (cat. no. NBP1-50051PE); 1:500; anti-AIPL1 (cat. no. 15108-1-AP), 1:500; anti-tubulin (cat. no. sc-5274, Santa Cruz Biotechnology, Inc.), 1:500; anti-human centromere CREST (cat. no. 15-234, Antibodies Incorporated), 1:500. Oocytes were examined using an Andor Revolution spinning disc confocal workstation (Oxford Instruments).

Western blotting

In total, 100 oocytes were dissolved in Laemmli sample buffer (Bio-Rad Laboratories, Inc.) containing protease inhibitors and boiled for 5 min before being subjected to 10% SDS-PAGE. The separated protein was transferred to a PVDF membrane, then blocked with TBST (TBS containing 0.05% Tween-20) containing 5% nonfat dried milk for 1 h at room temperature. Then the PVDF membrane was separated and incubated with the following main antibodies at 4°C overnight: mouse monoclonal anti-β-actin (cat. no. A5316-100) was diluted with a blocking buffer (TBS containing 0.05% Tween-20) at a ratio of 1:1000; rabbit anti-ZP3 (cat. no. AV35855) was diluted with a blocking buffer at a ratio of 1:500; mouse monoclonal anti-lamin A (133A2) (cat. no. ab8980) was diluted with a blocking buffer at a ratio of 1:2000; goat polyclonal prelamin A (C-20) (cat. no. sc-6214) was diluted with a blocking buffer at a ratio of 1:1000; mouse monoclonal anti-lamin C (EM-11) (cat. no. NBP1–50051PE) was diluted with a blocking buffer at a ratio of 1:1000; rabbit anti-AIPL1 (cat. no. 15108-1-AP) was diluted with a blocking buffer at a ratio of 1:2000; mouse

Table 2. DNA oligos for siRNA production

Target site	DNA templates
AIPL1 CDS 83–107[a]	Oligo 1: GGATCCTAATACGACTCACTATATCACTGGCTCTCGAGTGACCTTTCA[b]
	Oligo 2: AATGAAAGGTCACTCGAGAGCCAGTGATATAGTGAGTCGTATTAGGATCC[b]
	Oligo 3: GGATCCTAATACGACTCACTATATGAAAGGTCACTCGAGAGCCAGTGA[b]
	Oligo 4: AATCACTGGCTCTCGAGTGACCTTTCATATAGTGAGTCGTATTAGGATCC[b]
AIPL1 CDS 522–546[a]	Oligo 1: GGATCCTAATACGACTCACTATAGATGCAGGCGGTACCTCTTCTTCAT[b]
	Oligo 2: AAATGAAGAAGAGGTACCGCCTGCATCTATAGTGAGTCGTATTAGGATCC[b]
	Oligo 3: GGATCCTAATACGACTCACTATAATGAAGAAGAGGTACCGCCTGCATC[b]
	Oligo 4: AAGATGCAGGCGGTACCTCTTCTTCATTATAGTGAGTCGTATTAGGATCC[b]
AIPL1 CDS 680–704[a]	Oligo 1: GGATCCTAATACGACTCACTATAAGATGATCAACACCCTGATCCTCAA[b]
	Oligo 2: AATTGAGGATCAGGGTGTTGATCATCTTATAGTGAGTCGTATTAGGATCC[b]
	Oligo 3: GGATCCTAATACGACTCACTATTGAGGATCAGGGTGTTGATCATCT[b]
	Oligo 4: AAAGATGATCAACACCCTGATCCTCAATATAGTGAGTCGTATTAGGATCC[b]
AIPL1 CDS 781–805[a]	Oligo 1: GGATCCTAATACGACTCACTATACCAGGGATCGTGAAGGCCTACTATA[b]
	Oligo 2: AATATAGTAGGCCTTCACGATCCCTGGTATAGTGAGTCGTATTAGGATCC[b]
	Olgo 3: GGATCCTAATACGACTCACTATATATAGTAGGCCTTCACGATCCCTGG[b]
	Oligo 4: AACCAGGGATCGTGAAGGCCTACTATATATAGTGAGTCGTATTAGGATCC[b]
Control[c]	Oligo 1: GGATCCTAATACGACTCACTATACCTACGCCACCAATTTCGTTTT[b]
	Oligo 2: AAAAACGAAATTGGTGGCGTAGGTATAGTGAGTCGTATTAGGATCC[b]
	Oligo 3: GGATCCTAATACGACTCACTATAAAACGAAATTGGTGGCGTAGG[b]
	Oligo 4: AACCTACGCCACCAATTTCGTTTTATAGTGAGTCGTATTAGGATCC[b]

[a]The numbers are the starting and ending positions of the target sites in AIPL1 CDS (NM_053245.2 in NCBI).
[b]Two pairs of DNA oligos are required for each double-stand siRNA. Oligo 2 is complementary with oligo 1 except for an 'AA' overhang at the 5′ end; Oligo 3 is complementary with oligo 4 except for an 'AA' overhang at the 5′ end. In each oligo, gene-specific sequences are underlined, other sequences are for recognition and binding by T7 RNA polymerase.
[c]Control siRNA does not target to any mRNA sequence in mouse.

monoclonal anti-CDK1 (cat. no. 33-1800) was diluted with a blocking buffer at a ratio of 1:1000; rabbit polyclonal anti-phospho-CDK1 (Thr161) was diluted with a blocking buffer at a ratio of 1:2000; mouse monoclonal anti-cyclin B (D-1) (cat. no. sc-166210) was diluted with a blocking buffer at a ratio of 1:1000; rabbit polyclonal anti-phospho-cyclin B1 (Ser133) was diluted with a blocking buffer at a ratio of 1:1000. After washing in TBST, the membranes were incubated with HRP-conjugated rabbit anti-goat IgG, HRP-conjugated goat anti-mouse IgG (diluted with a blocking buffer to 1:1000) or HRP-conjugated goat anti-rabbit IgG (diluted with a blocking buffer to 1:1000) for 1 h at room temperature and then treated with ECL Plus Western Blotting Detection System (Vazyme). In the experiment, ImageJ 1.8.0 was used as data analysis software.

Image area measurement and fluorescence intensity

A series of images taken under the confocal laser microscope along the z-axis was imported into the ImageJ software and the images were superimposed by the z-stacks function of the software. the icon marked with 'line chart' in ImageJ software was selected to enclose the spindle outline with a closed line chart. The average fluorescence intensity in the line graph could be obtained using the shortcut key 'control + m'. The same method could measure the average fluorescence intensity of the background around the spindle. The former subtracts the latter, which is the average fluorescence intensity of spindle microtubules. The measurement was repeated three times and the average value taken.

Data analysis and statistics

All experiments were repeated at least three times. Measurements on confocal images were performed using ImageJ software (National Institutes of Health). Results were expressed as mean ± standard error of the mean (SEM). Multigroup comparisons of the means were carried out by one-way analysis of variance (ANOVA) test with post hoc contrasts using the Student–Newman–Keuls test. A P-value < 0.05 was considered to indicate a significant difference.

The measurement method of ImageJ software is as follows. A series of images taken along the z-axis under the confocal laser microscope were imported into ImageJ software, in which the GV outline was enclosed and the average fluorescence intensity in the contour was measured. The same method can measure the average fluorescence intensity of the background around the GV area. The former subtracts the latter, which is the average fluorescence intensity of the GV area. The measurement was repeated three times and the average value taken.

Results

There were no significant changes in the expression, phosphorylation and cell distribution of MPF in ZP3-deficient oocytes. Our previous studies have shown that there was a significant decrease in the GVBD rate after ZP3 was knocked down by specific siRNA (Gao *et al.*, 2017). The current study showed that, after the knockdown of ZP3 and development *in vitro*, the contents of MPF
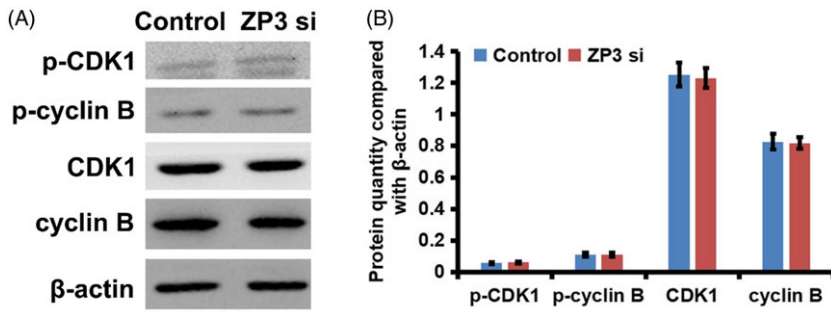
Figure 1. (A) There were no significant changes in the expression, phosphorylation and cell distribution of MPF in ZP3-deficient oocytes. Western blot showed that when ZP3 was knocked down by specific siRNA, the levels of CDK-1, p-CDK-1, cyclin B and p-cyclin B did not change significantly. (B) Measurement and statistics of western blots also illustrates this point. β-Actin was used as a control. *$P < 0.05$ was considered to indicate a statistically significant difference. In total, 100 oocytes were used in each group. Three independent experiments were performed for each result.
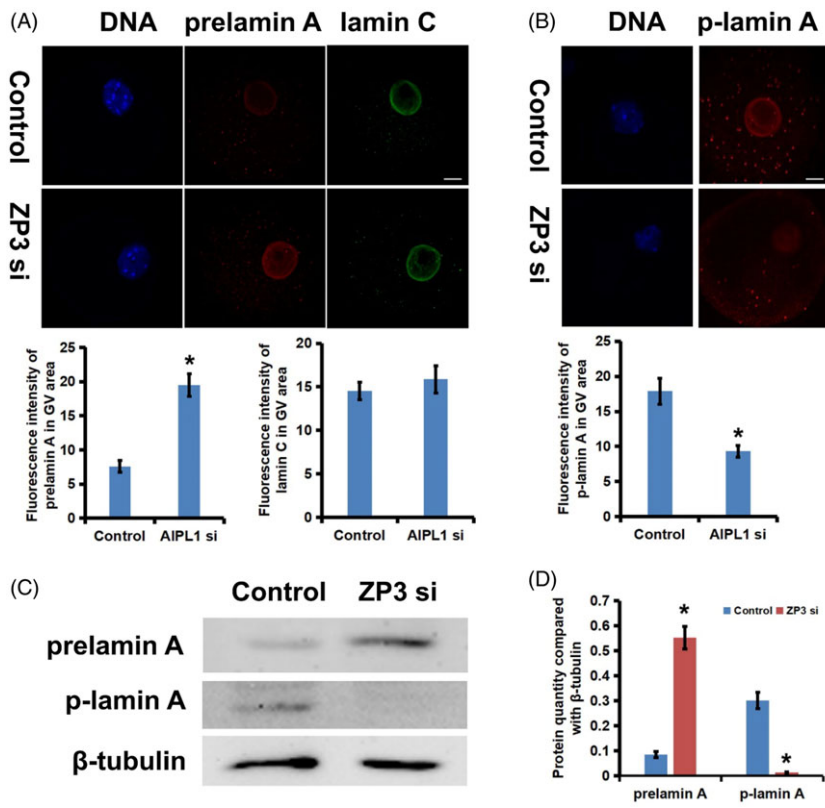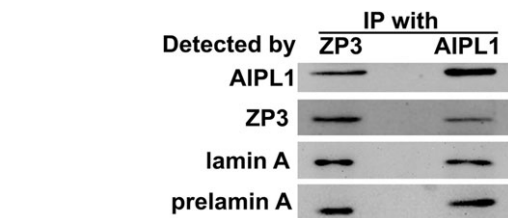

Figure 2. In ZP3-deficient oocytes, prelamin A could not mature and accumulated in the nucleus. Immature prelamin A could not be phosphorylated, resulting in the decrease in p-lamin A. (A) Immunofluorescence showed that in ZP3 lacking oocytes, prelamin A increased significantly in the nuclear membrane and nucleus, while the distribution of lamin C did not appear to change. The measurement and statistics of prelamin A and lamin C fluorescence intensity in the GV region of oocytes also illustrate this point. DNA is displayed in blue, prelamin A in red and lamin C in green. (B) Immunofluorescence showed that p-lamin A decreased clearly in oocytes with ZP3 deleted. The measurement and statistics of p-lamin A fluorescence intensity in the GV region of oocytes also illustrate this point. DNA is displayed in blue and p-lamin A in red. (C) Western blot showed that, when ZP3 was specifically knocked down, prelamin A increased markedly, while p-lamin A decreased significantly. β-Actin was used as a control. (D) Measurement and statistics of western blots also prove this point. Scale bar, 20 μm. *$P < 0.05$ was considered to indicate a statistically significant difference. In total, 100 oocytes were used in each group. Three independent experiments were performed for each result.

Figure 3. ZP3 and AIPL1 interact with lamin A and prelamin A. The co-IP experiment shows that ZP3 antibody could precipitate AIPL1, lamin A and prelamin A. AIPL1 antibody could precipitate ZP3, lamin A and prelamin A. In total, 300 oocytes were used in each group. Three independent experiments were performed for each result.

(CDK1 and cyclin B) and their phosphorylation levels did not change significantly (Figure 1A,B). This showed that ZP3 deletion affected the occurrence of GVBD, which was not realized by affecting the activation of MPF.

In ZP3-deficient oocytes, prelamin A could not mature and accumulated in the nucleus. Immature prelamin A could not be phosphorylated, resulting in a decrease in p-lamin A. Our previous studies showed that lamin A mainly accumulated in the nuclear membrane of GV oocytes. When ZP3 was knocked down, the distribution of lamin A in the nucleus of oocytes increased significantly and the distribution of the nuclear membrane decreased (Gao *et al.*, 2017). Immunofluorescence (Figure 2A, B) and western blot (Figure 2C,D) analyses showed that, in ZP3-deficient oocytes, prelamin A increased significantly in the nuclear membrane and nucleus, whereas p-lamin A decreased significantly. Knockdown of ZP3 did not change the distribution of lamin C in the oocytes (Figure 2A). These results suggested that when oocytes lack ZP3, the accuracy of prelamin A binding to the nuclear membrane decreases, and prelamin A on the nuclear membrane and nucleus cannot continue to process into mature lamin A. Immature prelamin A cannot be phosphorylated by MPF, resulting in the decrease in p-lamin A and an obstacle to GVBD.

ZP3 and AIPL1 interacted with lamin A and prelamin A. Our previous studies have demonstrated that when the oocyte samples with the zona pellucida removed were used for immunoprecipitation (IP) experiments, possible interacting proteins aryl hydrocarbon receptor-interacting protein-like 1 (AIPL1) and lamin A were

Figure 4. AIPL1 deficiency leads to the GVBD disorder in oocytes, accompanied by the accumulation of prelamin A, the decrease of p-lamin A and the abnormal distribution of ZP3. (A, C) When AIPL1 was knocked down, prelamin A increased markedly, while p-lamin A decreased significantly. Measurement and statistics of western blots also illustrate this point. β-Actin was used as a control. (B, D) When AIPL1 was knocked down, the expression of AIPL1 was decreased obviously, while the level of ZP3 showed no significant change. Measurement and statistics of western blots also illustrate this point. β-Actin was used as a control. (E, F) Immunofluorescence showed that in AIPL1-lacking oocytes, ZP3 in the germinal vesicle area of oocytes remained unchanged. The measurement and statistics of ZP3 fluorescence intensity in the GV region of oocytes also illustrate this point. DNA is displayed in blue and ZP3 in green. Scale bar, 20 μm. (G, H) *In vitro* development of oocytes and related statistical analysis showed that the ratio of GVBD of oocytes lacking AIPL1 decreased significantly after 2 h of *in vitro* development. Scale bar, 100 μm. *A P-value < 0.05 was considered to indicate a statistically significant difference. In total, 100 oocytes were fixed and stained in each group, and the number and proportion of chromosomal abnormalities in each group were assessed. Three independent experiments were performed for each result.
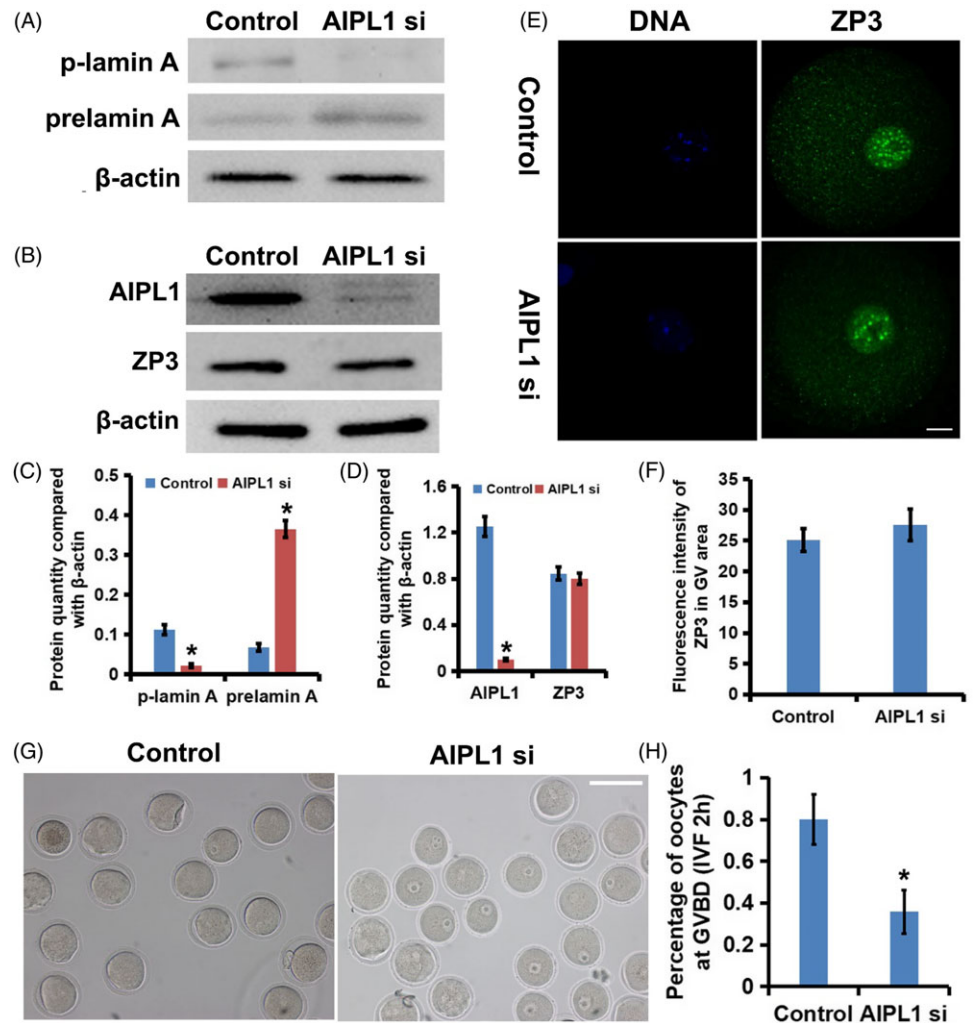
detected (Gao *et al.*, 2017). Our co-IP experiment shows that ZP3 interacted with AIPL1, lamin A and prelamin A (Figure 3). AIPL1 antibody can also precipitate lamin A and prelamin A, indicating their interaction (Figure 3).

AIPL1 deficiency leads to a GVBD disorder in oocytes, accompanied by the accumulation of prelamin A, the decrease in p-lamin A, and the abnormal distribution of ZP3. Our previous studies have shown that AIPL1 was also located in the oocyte GV, and ZP3 knockdown significantly inhibited the aggregation of AIPL1 in this region (Gao *et al.*, 2017). When AIPL1 was knocked down, the expression of ZP3 (Figure 4B,D) and its distribution (Figure 4E, F) in the GV area of oocytes remained unchanged. However, similar to ZP3 knockdown, the deletion of AIPL1 led to the arrest of GVBD in oocytes (Figure 4G,H), and also caused an increase in prelamin A and a decrease in p-lamin A (Figure 4A,C). Combined with the effect of ZP3 on the nuclear localization of AIPL1, it is speculated that ZP3 on the nuclear membrane may bind and activate AIPL1, promoting the maturation and phosphorylation of lamin A, and then promoting the occurrence of GVBD.

Our study enriched the model of oocyte GVBD. Combined with our current research and the known mechanism of GVBD, we speculate that, in GV oocytes, prelamin A is bound to the nuclear membrane after farnesylation modification. ZP3 on the nuclear membrane binds and activates AIPL1 to stabilize farnesylated prelamin A on the nuclear membrane and promote its processing into mature lamin A, which can be phosphorylated and decomposed by MPF, resulting in the occurrence of GVBD (Figure 5A). When oocytes lack ZP3, AIPL1 cannot be activated, farnesylated prelamin A on the nuclear membrane cannot be bound, and cannot be processed into mature lamin A. The phosphorylation disorder of lamin A leads to a disorder of GVBD (Figure 5B). At this time, the abnormality in prelamin A caused by the composition change and instability of the nuclear membrane may also be another factor for GVBD disorder (Figure 5B).

Discussion

ZP3 is an important component of the zona pellucida of oocytes, and can act as a primary sperm receptor and induce the acrosome reaction during fertilization (Gupta, 2018; Wassarman and Litscher, 2018). ZP3 knockout mice lose fertility completely (Liu *et al.*, 1996). Recent studies have found that ZP3 mutation can lead to oocyte development disorder. In 2017, the research team of Professor Chen Zi-Jiang of Shandong University found that the ZP3 c.400 G>A (p.Ala134Thr) heterozygous missense mutation may be the pathogenic mutation of empty follicle syndrome (EFS), providing a potential diagnostic target for EFS (Chen *et al.*, 2017). It is believed that zona pellucida-related defects caused by ZP3 mutation lead to oocyte development disorder and eventually degeneration, resulting in the empty follicle phenomenon.
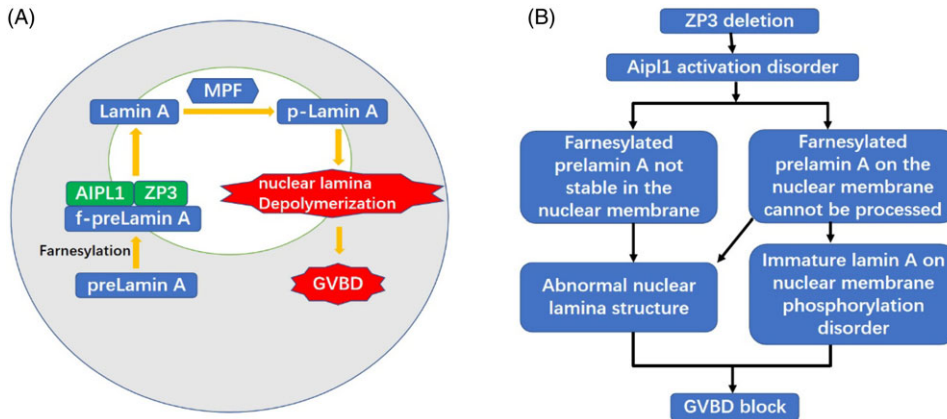
(A)

(B)

Figure 5. Our study enriched the model of oocyte GVBD. (A) Combined with our current research and the known mechanism of GVBD, we speculate that in GV oocytes, prelamin A is bound to the nuclear membrane after farnesylation modification. ZP3 on the nuclear membrane binds and activates AIPL1 to stabilize farnesylated prelamin A on the nuclear membrane and promote its processing into mature lamin A, which can be phosphorylated and decomposed by MPF, resulting in the occurrence of GVBD. (B) When oocytes lack ZP3, AIPL1 cannot be activated, farnesylated prelamin A on the nuclear membrane cannot be bound, and cannot be processed into mature lamin A. The phosphorylation disorder of lamin A leads to the GVBD disorder. At this time, the abnormality for prelamin A caused by the composition change and instability of nuclear membrane may also be another factor in the GVBD disorder.

The related mechanism of oocyte development and maturation of EFS has not been much discussed (Chen *et al.*, 2017).

Our previous study found that ZP3 was located not only in zona pellucida, but also in the nucleus of GV oocytes. However, in GVBD and subsequent oocytes, it decreased significantly around chromosomes (Gao *et al.*, 2017). When ZP3 was knocked down by specific siRNA, the oocyte development was obviously impaired, and the percentage of oocytes arrested in GV phase was significantly increased, suggesting that ZP3 may play an important role in the development of GVBD (Gao *et al.*, 2017). Western blot showed that the expression and phosphorylation of MPF (including cyclin B and CDK1) did not change significantly after ZP3 was knocked down by specific siRNA, indicating that the mechanism of ZP3 affecting GVBD may be a downstream pathway of MPF. Immunoprecipitation (IP) experiments were carried out on oocyte samples with the zona pellucida removed, and possible interacting proteins AIPL1 and lamin A were detected.

Lamin A/C is produced by the *LMNA* gene located on chromosome lq21.2–q21.3. The gene encodes different protein products by selective splicing of 12 exons, among which lamin A and lamin C are the main products (Liu and Zhou, 2008). Lamin C and lamin A have the same 566 amino acid residues at the N-terminal. In the subsequent amino acid sequences, lamin C lost part of exon 10 and all of exons 11 and 12, but had six specific amino acid residues at the C-terminal. Lamin A is synthesized in the form of a precursor protein, called prelamin A. It has a carboxyl tail of 98 special amino acids, and its C-terminal contains CaaX (C is cysteine; a is aliphatic amino acid. X is variable amino acid) motif. During the maturation of lamin, the cysteine side chain of the CaaX motif is first modified by farnesylation, which makes prelamin A gain a non-polar farnesylation group, and which can help prelamin A bind more easily to the nuclear membrane. When prelamin A migrates to the nuclear membrane, the '–AAX' in its CaaX motif is removed by metalloproteinase Zmpste24 and/or endopeptidase Rce1. The exposed farnescysteine is methylated by isoprenylcysteine carboxyl methyltransferase (ICMT) in the endoplasmic reticulum. Finally, the final 15 amino acid residues (including farnesyl methyl ester) of prelamin A are removed by Zmpste24 again, and mature lamin A is finally formed (Peter *et al.*, 1991; Delbarre *et al.*, 2006; Meta *et al.*, 2006; Young *et al.*, 2006).

Studies on somatic cells have shown that farnesylation of prelamin A is a key step in its localization to the nuclear membrane (Peter *et al.*, 1991; Barrowman *et al.*, 2008; Taimen *et al.*, 2009; Moiseeva *et al.*, 2016). When the farnesylated prelamin A was localized to the nuclear membrane, it was further modified to form mature lamin A (Meta *et al.*, 2006; Young *et al.*, 2006; Liu and Zhou, 2008). In human U2OS cell lines, when prelamin A is abnormally farnesylated and cannot form mature lamin A, the phosphorylation of its 22nd serine will be inhibited, and nuclear membrane rupture will also be affected (Peter *et al.*, 1990). Mutation in the human *LMNA* gene means that prelamin A lacks the Zmpste24 splicing site. Farnesylated prelamin A cannot be normally processed into mature lamin A and accumulates in the nuclear membrane, which affects the integrity of the nuclear membrane, resulting in an abnormal nuclear shape, and finally leads to Hutchinson–Gilford progeria syndrome (HGPS) (De Sandre-Giovannoli *et al.*, 2003; Eriksson *et al.*, 2003; Hennekam, 2006). Recent studies have shown that the abnormal nuclear shape was reduced after treatment with a farnesyl transferase inhibitor (FTI) (Yang *et al.*, 2006; Hernandez *et al.*, 2010; Larrieu *et al.*, 2014). The process and regulatory mechanism of farnesylation of prelamin A in oocytes have not been reported.

Immunofluorescence showed that lamin A was mainly concentrated in the nuclear membrane. When ZP3 was knocked down, the distribution of lamin A in the nucleus increased significantly, the distribution of the nuclear membrane decreased to a certain extent, and the amount of prelamin A in both the nuclear membrane and nucleus increased significantly. Western blot showed that the amount of prelamin A increased significantly, whereas phosphorylated lamin A (p-lamin A) decreased significantly. Knockdown of ZP3 did not change the distribution of lamin C in oocytes. These results suggested that when ZP3 was absent in oocytes, the accuracy of binding prelamin A to the nuclear membrane was reduced, and prolamin A on the nuclear membrane cannot be processed into mature lamin A, which leads to the GVBD failure.

AIPL1 is a specific partner of visual effector phosphodiesterase-6 (PDE6). The results show that AIPL1 can bind to the farnesylated PDE6a subunit and maintain its stability (Liu *et al.*, 2004; Ramamurthy *et al.*, 2004; Larrieu *et al.*, 2014). Molecular experiments *in vitro* also showed that the binding site of AIPL1 was in the farnesyl group (Majumder *et al.*, 2013). AIPL1 mutation destroys the stability of PDE6 and leads to Leber congenital amaurosis type 4 (LCA4) (Dharmaraj *et al.*, 2004; Ramamurthy *et al.*, 2004). As a molecular chaperone, AIPL1 can specifically interact with farnesylated proteins (Ramamurthy *et al.*, 2003). By combining with each other, AIPL1 is very important for the stability and fate of farnesylated protein, which can avoid protein degradation

and promote its further processing (Ramamurthy *et al.*, 2004). Whether AIPL1 regulates the farnesylation of prelamin A or whether AIPL1 plays a role in the meiotic recovery of oocytes has not been reported. As mentioned above, the farnesylation of prelamin A is a key step in promoting its localization to the nuclear membrane. Moreover, in human U2OS cell lines, the abnormal processing of prelamin A inhibits its serine phosphorylation at position 22, which is necessary for nuclear fibre layer decomposition and nuclear membrane rupture.

Immunofluorescence showed that AIPL1 was also located in the GV nuclear region of oocytes, and ZP3 knockdown could significantly inhibit the aggregation of AIPL1 in the nuclear region. When AIPL1 was knocked down, the expression of ZP3 and its localization in the oocyte nucleus did not change but, similar to ZP3 knockdown, the deletion of AIPL1 led to the decrease of the incidence of GVBD in oocytes, the increase in prelamin A and the significant decrease of p-lamin A. Combined with the effects of ZP3 on the nuclear localization of AIPL1, it is speculated that ZP3 on the nuclear membrane may activate it by binding to AIPL1, and promote the occurrence of GVBD by promoting the maturation and phosphorylation of lamin A. In addition, the experiments also showed that the nuclear localization of ZP3 was not affected by AIPL1, and the regulation mechanism of its localization needs to be further studied.

We speculate that ZP3 may promote binding of AIPL1, stabilize the farnesylated prelamin A on the nuclear membrane, and promote its further processing into mature lamin A, which can be phosphorylated and decomposed by MPF, leading to the occurrence of GVBD. When ZP3 is absent in oocytes, AIPL1 cannot be activated, which leads to the failure of binding of farnesylated prelamin A on the nuclear membrane, which cannot be processed into mature lamin A. the phosphorylation of the latter leads to the GVBD disorder. At this time, the unstable farnesylated prelamin A on the nuclear membrane can migrate into the nucleus without accumulating at the nuclear membrane, resulting in an abnormal karyotype. However, the abnormality of the nuclear fibre layer caused by this instability and composition change may also be another factor in GVBD disorder.

At present, the mode of nuclear localization and specific interaction between ZP3 and AIPL1, the mechanism and regulation mode of AIPL1 participating in farnesylation of prelamin A to stabilize the nuclear membrane and further process to mature lamin A need further verification and more detailed in-depth study. If the mode of action can be proved, it will be an important supplement to provide a new diagnostic target and treatment clue for patients with oocyte maturation disorder in assisted reproduction.

In conclusion, this study reveals that both ZP3 and AIPL1 are strongly concentrated in the nuclear region of GV-stage oocytes, and both interact with lamin A localized in the nuclear membrane. ZP3 may cooperate with AIPL1 to stabilize farnesylated prelamin A on the nuclear membrane and promote its further processing into mature lamin A, therefore promoting the occurrence of GVBD. This study may make an important contribution to the mechanism of oocyte GVBD and provide new diagnostic targets and therapeutic clues for infertile patients with oocyte maturation disorders.

References

Adhikari, D., Zheng, W., Shen, Y., Gorre, N., Ning, Y., Halet, G., Kaldis, P. and Liu, K. (2012). Cdk1, but not Cdk2, is the sole Cdk that is essential and sufficient to drive resumption of meiosis in mouse oocytes. *Human Molecular Genetics*, **21**(11), 2476–2484. doi: 10.1093/hmg/dds061

Barrowman, J., Hamblet, C., George, C. M. and Michaelis, S. (2008). Analysis of prelamin A biogenesis reveals the nucleus to be a CaaX processing compartment. *Molecular Biology of the Cell*, **19**(12), 5398–5408. doi: 10.1091/mbc.e08-07-0704

Chen, T., Bian, Y., Liu, X., Zhao, S., Wu, K., Yan, L., Li, M., Yang, Z., Liu, H., Zhao, H. and Chen, Z. J. (2017). A recurrent missense mutation in ZP3 causes empty follicle syndrome and female infertility. *American Journal of Human Genetics*, **101**(3), 459–465. doi: 10.1016/j.ajhg.2017.08.001

De Sandre-Giovannoli, A., Bernard, R., Cau, P., Navarro, C., Amiel, J., Boccaccio, I., Lyonnet, S., Stewart, C. L., Munnich, A., Le Merrer, M. and Lévy, N. (2003). Lamin a truncation in Hutchinson-Gilford progeria. *Science*, **300**(5628), 2055. doi: 10.1126/science.1084125

Dechat, T., Pfleghaar, K., SenGupta, K., Shimi, T., Shumaker, D. K., Solimando, L. and Goldman, R. D. (2008). Nuclear lamins: Major factors in the structural organization and function of the nucleus and chromatin. *Genes and Development*, **22**(7), 832–853. doi: 10.1101/gad.1652708

Delbarre, E., Tramier, M., Coppey-Moisan, M., Gaillard, C., Courvalin, J. C. and Buendia, B. (2006). The truncated prelamin A in Hutchinson–Gilford progeria syndrome alters segregation of A-type and B-type lamin homopolymers. *Human Molecular Genetics*, **15**(7), 1113–1122. doi: 10.1093/hmg/ddl026

Dessev, G., Iovcheva-Dessev, C., Bischoff, J. R., Beach, D. and Goldman, R. (1991). A complex containing p34cdc2 and cyclin B phosphorylates the nuclear lamin and disassembles nuclei of clam oocytes *in vitro*. *Journal of Cell Biology*, **112**(4), 523–533. doi: 10.1083/jcb.112.4.523

Dharmaraj, S., Leroy, B. P., Sohocki, M. M., Koenekoop, R. K., Perrault, I., Anwar, K., Khaliq, S., Devi, R. S., Birch, D. G., De Pool, E., Izquierdo, N., Van Maldergem, L., Ismail, M., Payne, A. M., Holder, G. E., Bhattacharya, S. S., Bird, A. C., Kaplan, J. and Maumenee, I. H. (2004). The phenotype of Leber congenital amaurosis in patients with AIPL1 mutations. *Archives of Ophthalmology*, **122**(7), 1029–1037. doi: 10.1001/archopht.122.7.1029

Eriksson, M., Brown, W. T., Gordon, L. B., Glynn, M. W., Singer, J., Scott, L., Erdos, M. R., Robbins, C. M., Moses, T. Y., Berglund, P., Dutra, A., Pak, E., Durkin, S., Csoka, A. B., Boehnke, M., Glover, T. W. and Collins, F. S. (2003). Recurrent *de novo* point mutations in lamin A cause

Hutchinson-Gilford progeria syndrome. *Nature*, **423**(6937), 293–298. doi: 10.1038/nature01629

Gao, L. L., Zhou, C. X., Zhang, X. L., Liu, P., Jin, Z., Zhu, G. Y., Ma, Y., Li, J., Yang, Z. X. and Zhang, D. (2017). ZP3 is required for germinal vesicle breakdown in mouse oocyte meiosis. *Scientific Reports*, **7**, 41272. doi: 10.1038/srep41272

Gupta, S. K. (2018). The human egg's zona Pellucida. *Current Topics in Developmental Biology*, **130**, 379–411. doi: 10.1016/bs.ctdb.2018.01.001

Hennekam, R. C. (2006). Hutchinson-Gilford progeria syndrome: Review of the phenotype. *American Journal of Medical Genetics. Part A*, **140**(23), 2603–2624. doi: 10.1002/ajmg.a.31346.

Hernandez, L., Roux, K. J., Wong, E. S., Mounkes, L. C., Mutalif, R., Navasankari, R., Rai, B., Cool, S., Jeong, J. W., Wang, H., Lee, H. S., Kozlov, S., Grunert, M., Keeble, T., Jones, C. M., Meta, M. D., Young, S. G., Daar, I. O., Burke, B.,... Stewart, C. L. (2010). Functional coupling between the extracellular matrix and nuclear lamina by Wnt signalling in progeria. *Developmental Cell*, **19**(3), 413–425. doi: 10.1016/j.devcel.2010.08.013

Larrieu, D., Britton, S., Demir, M., Rodriguez, R. and Jackson, S. P. (2014). Chemical inhibition of NAT10 corrects defects of laminopathic cells. *Science*, **344**(6183), 527–532. doi: 10.1126/science.1252651

Liu, B. and Zhou, Z. (2008). Lamin A/C, laminopathies and premature ageing. *Histology and Histopathology*, **23**(6), 747–763. doi: 10.14670/HH-23.747

Liu, C., Litscher, E. S., Mortillo, S., Sakai, Y., Kinloch, R. A., Stewart, C. L. and Wassarman, P. M. (1996). Targeted disruption of the *mZP3* gene results in production of eggs lacking a zona pellucida and infertility in female mice. *Proceedings of the National Academy of Sciences of the United States of America*, **93**(11), 5431–5436. doi: 10.1073/pnas.93.11.5431

Liu, X., Bulgakov, O. V., Wen, X. H., Woodruff, M. L., Pawlyk, B., Yang, J., Fain, G. L., Sandberg, M. A., Makino, C. L. and Li, T. (2004). AIPL1, the protein that is defective in Leber congenital amaurosis, is essential for the biosynthesis of retinal rod cGMP phosphodiesterase. *Proceedings of the National Academy of Sciences of the United States of America*, **101**(38), 13903–13908. doi: 10.1073/pnas.0405160101

Majumder, A., Gopalakrishna, K. N., Cheguru, P., Gakhar, L. and Artemyev, N. O. (2013). Interaction of aryl hydrocarbon receptor-interacting protein-like 1 with the farnesyl moiety. *Journal of Biological Chemistry*, **288**(29), 21320–21328. doi: 10.1074/jbc.M113.476242

Mehsen, H., Boudreau, V., Garrido, D., Bourouh, M., Larouche, M., Maddox, P. S., Swan, A. and Archambault, V. (2018). PP2A-B55 promotes nuclear envelope reformation after mitosis in *Drosophila*. *Journal of Cell Biology*, **217**(12), 4106–4123. doi: 10.1083/jcb.201804018

Meta, M., Yang, S. H., Bergo, M. O., Fong, L. G. and Young, S. G. (2006). Protein farnesyltransferase inhibitors and progeria. *Trends in Molecular Medicine*, **12**(10), 480–487. doi: 10.1016/j.molmed.2006.08.006

Moiseeva, O., Lopes-Paciencia, S., Huot, G., Lessard, F. and Ferbeyre, G. (2016) Permanent farnesylation of lamin A mutants linked to progeria impairs its phosphorylation at serine 22 during interphase. *Aging*, **8**(2), 366–381. doi: 10.18632/aging.100903

Peter, M., Nakagawa, J., Dorée, M., Labbé, J. C. and Nigg, E. A. (1990). *In vitro* disassembly of the nuclear lamina and M phase-specific phosphorylation of lamins by cdc2 kinase. *Cell*, **61**(4), 591–602. doi: 10.1016/0092-8674(90)90471-p

Peter, M., Heitlinger, E., Häner, M., Aebi, U. and Nigg, E. A. (1991). Disassembly of *in vitro* formed lamin head-to-tail polymers by CDC2 kinase. *EMBO Journal*, **10**(6), 1535–1544. doi: 10.1002/j.1460-2075.1991.tb07673.x

Ramamurthy, V., Roberts, M., van den Akker, F., Niemi, G., Reh, T. A. and Hurley, J. B. (2003). AIPL1, a protein implicated in Leber's congenital amaurosis, interacts with and aids in processing of farnesylated proteins. *Proceedings of the National Academy of Sciences of the United States of America*, **100**(22), 12630–12635. doi: 10.1073/pnas.2134194100

Ramamurthy, V., Niemi, G. A., Reh, T. A. and Hurley, J. B. (2004). Leber congenital amaurosis linked to AIPL1: A mouse model reveals destabilization of cGMP phosphodiesterase. *Proceedings of the National Academy of Sciences of the United States of America*, **101**(38), 13897–13902. doi: 10.1073/pnas.0404197101

Taimen, P., Pfleghaar, K., Shimi, T., Möller, D., Ben-Harush, K., Erdos, M. R., Adam, S. A., Herrmann, H., Medalia, O., Collins, F. S., Goldman, A. E. and Goldman, R. D. (2009). A progeria mutation reveals functions for lamin A in nuclear assembly, architecture, and chromosome organization. *Proceedings of the National Academy of Sciences of the United States of America*, **106**(49), 20788–20793. doi: 10.1073/pnas.0911895106

Wassarman, P. M. and Litscher, E. S. (2018). The mouse egg's zona Pellucida. *Current Topics in Developmental Biology*, **130**, 331–356. doi: 10.1016/bs.ctdb.2018.01.003

Yang, S. H., Meta, M., Qiao, X., Frost, D., Bauch, J., Coffinier, C., Majumdar, S., Bergo, M. O., Young, S. G. and Fong, L. G. (2006). A farnesyltransferase inhibitor improves disease phenotypes in mice with a Hutchinson-Gilford progeria syndrome mutation. *Journal of Clinical Investigation*, **116**(8), 2115–2121. doi: 10.1172/JCI28968

Young, S. G., Meta, M., Yang, S. H. and Fong, L. G. (2006). Prelamin A farnesylation and progeroid syndromes. *Journal of Biological Chemistry*, **281**(52), 39741–39745. doi: 10.1074/jbc.R600033200